Sensors and Materials, Vol. 38, No. 7 (2026) 4183–4194
MYU Tokyo

S & M 4557

Real-time Monitoring of CO_2 Capture and Syngas Production Using Integrated Sensing Systems and Waste Platinum Catalyst

Chih Ju G. Jou[1*] and Chienli Lee[2]

[1]Department of Safety, Health and Environmental Engineering,
National Kaohsiung University of Science and Technology, 824, Taiwan
[2]Research and Development Center for Water Resource and Conservation,
National Kaohsiung University of Science and Technology, 824, Taiwan

(Received May 11, 2026; accepted July 1, 2026)

Keywords: carbon capture, waste catalyst, syngas, microwave energy

For carbon capture and utilization, real-time monitoring technologies are employed in syngas production through efficient CO_2 capture and conversion, achieving a synergistic relationship between chemical process control and sensor performance. An alkaline absorption system was developed to capture CO_2 (14500–14800 ppm), which was subsequently converted into syngas using waste platinum (Pt) catalysts via microwave induction. Integrated sensing systems, including nondispersive infrared sensors and electrochemical probes, were employed to quantify CO_2 capture kinetics and evaluate process stability. Increasing the NaOH concentration from 1 to 7% extended the CO_2 breakthrough time from 138 to 1782 s. High-resolution sensors enabled the identification of ionic conductivity signatures, where the 3.6-fold difference in equivalent conductivity between OH^- and CO_3^{2-} facilitated the predictive monitoring of solvent exhaustion. Microwave-assisted dry reforming (450 W) using 6 g of waste Pt catalyst and 0.8 g of micron-sized iron powder achieved average H_2 and CO yields of 18.8 and 25.1%, respectively. The results demonstrate that integrated sensor networks are essential for managing the inherent variability of CO_2 absorption, thereby enabling an automated, sensor-driven circular economy.

1. Introduction

Among greenhouse gases, carbon dioxide (CO_2) has made a significant contribution to global warming. Atmospheric CO_2 concentration has reached the highest level ever recorded (>400 ppm).[1,2] Therefore, reducing atmospheric CO_2 emissions has become a major environmental challenge for mitigating the effects of global warming.[3,4] Carbon capture and storage (CCS) technology is one of the effective approaches for reducing greenhouse gas emissions and mitigating global warming.[5] In addition to CCS technology, carbon capture and utilization (CCU) technology has also attracted significant research interest, as CCU does not require long-term storage facilities, unlike CCS. Therefore, CCU is regarded as a cost-effective option for reducing greenhouse gas emissions, as the costs of CO_2 capture can be offset by the value of

*Corresponding author: e-mail: george@nkust.edu.tw
https://doi.org/10.18494/SAM6412

ISSN 0914-4935

products generated through CCU processes. In CCU, captured CO_2 is converted into commercially valuable materials, such as construction materials, through a chemical mineralization process.[6]

Unlike CCS, which involves the energy-intensive compression, transportation, and long-term geological storage of captured CO_2, CCU focuses on converting captured CO_2 into value-added products, thereby providing potential economic benefits while reducing dependence on fossil-based resources. Therefore, CCU is considered a promising approach for promoting a circular carbon economy, as the economic value generated from CO_2-derived products may partially compensate for the CO_2 capture and conversion costs. In CCU processes, captured CO_2 can be transformed into commercially valuable products, such as fuels, chemicals, and construction materials, through various pathways including catalytic conversion and mineralization.[6] However, the overall environmental benefits of CCU strongly depend on the energy source, conversion efficiency, product utilization, and life-cycle carbon emissions associated with the process.

For CO_2 capture, physical or chemical absorption methods are employed. Chemical absorption is generally preferred over physical absorption because the chemical reaction, involving acid–base neutralization with amine (NH_3-based) solvents, significantly enhances the mass transfer and diffusion of CO_2 into the liquid phase. This process overcomes the inherent kinetic and thermodynamic limitations associated with physical absorption, such as low absorption capacity at low partial pressures, slow reaction kinetics, and poor selectivity in the presence of competing gas species. Chemical absorption using sodium hydroxide (NaOH) has been recognized as one of the most widely implemented technologies in CCS. The mechanism involves a reversible chemical reaction between CO_2 and NaOH, followed by regeneration through thermal treatment. One of the advantages of using NaOH solutions in chemical CO_2 absorption is the potential integration of renewable energy sources into NaOH production.[7]

In the chemical process, conductivity-based concentration monitoring using sensors is essential for maintaining process efficiency and evaluating solvent degradation. The advancement of CCS technology has become closely linked with the development of high-precision sensor networks. Sensors play an important role in quantifying capture efficiency, monitoring catalyst degradation, and ensuring the safety of sequestration sites.[8] In CO_2 capture processes, sensor technology enables a real-time feedback loop for optimizing gas-to-catalyst ratios and thermal conditions.

In this study, an alkaline solution was employed as the CO_2 absorption medium for carbon capture. CO_2 was subsequently converted into syngas through a catalytic thermochemical reaction using waste-derived Pt catalysts with a carbon content of approximately 1.4 wt% under microwave irradiation. Sensors play a critical role in quantifying capture efficiency, monitoring catalyst degradation, and ensuring the safety of sequestration sites.[8] In the developed process, sensor technology is used to mitigate unpredictable reaction kinetics caused by impurities associated with recycled Pt catalysts. Sensors address this challenge by providing the continuous monitoring of chemical stability, catalyst surface activity, and capture rates, thereby advancing previous catalytic approaches toward automated, high-efficiency systems.[9] Moreover, sensors enable the adaptive control of microwave-induced heating, ensuring uniform temperature

distribution and preventing localized catalyst degradation, which has been reported as a major limitation in previous chemical absorption methods.[10] By integrating sensor technology into the CO_2 conversion system, catalytic performance is systematically monitored to enhance safety and industrial process control. This integration improves production efficiency and facilitates the scalability of circular carbon utilization in industrial applications.[11]

2. Methods

2.1 Carbon capture equipment

The alkali carbon capture system consists of an alkali solution blending tank (320 × 550 × 147 mm), a diaphragm pump (maximum pressure: 8.5 bar; flow rate: 2.0 L/min), mass flow controllers (MFCs), and a DC 24 V/1.3 A power supply. As shown in Fig. 1, the prepared alkali absorption solution is stored in the blending tank and circulated through the absorption loop by the diaphragm pump.The alkali solution is continuously delivered to the gas–liquid absorption unit (38.1 mm outer diameter × 365 mm length), where it contacts the CO_2 containing gas introduced from the bottom inlet. The gas flow rate is regulated by the MFCs, and the gas–liquid interaction within the absorption unit promotes CO_2 dissolution and reaction with the alkaline solution. After absorption, the liquid phase flows back to the absorbent circulation surge tank, maintaining continuous circulation and stable operation. The treated gas exits through the upper outlet and passes through the gas sampling point, where the CO_2 concentration is measured using the NDIR sensor. The conductivity sensor is used to monitor variations in the alkaline solution during circulation. The CO_2 absorption efficiency is determined on the basis of the difference between the inlet and outlet CO_2 concentrations; the simple system layout is shown in Fig. 1. Synthesis gas (syngas) production is conducted using a laboratory-scale microwave oven (MOB-P23, SAMPO, China) equipped with a proportional, integral, and derivative (PID) control system to regulate microwave output power. Syngas is a fuel gas mixture consisting of hydrogen

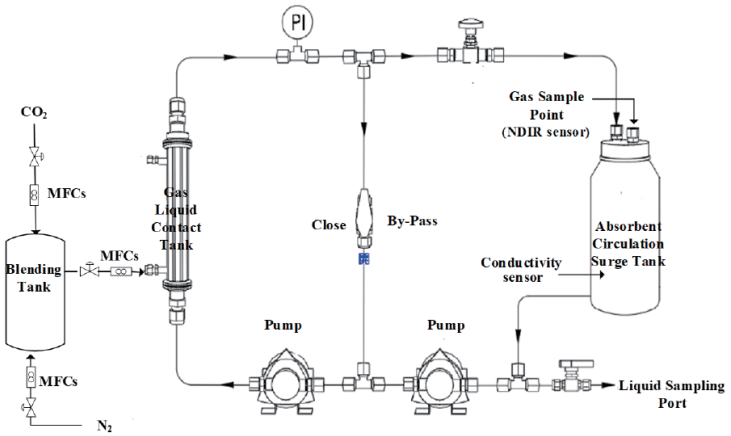

Fig. 1. (Color online) Diagram of alkali carbon capture equipment [PI: pressure indicator (gauge); NDIR: nondispersive infrared sensor].

(H_2), carbon monoxide, and CO_2. It is an essential intermediate because it acts as a building block that can be converted into a wide range of fuels and chemicals. Syngas is a valuable product generated from the catalytic reforming of CH_4 and CO_2 using waste platinum catalyst.

The microwave oven operates at 2.45 GHz with a maximum output of 850 W. A custom-made 100 mL cylindrical quartz vessel with micropores (40 pores, 1 mm diameter) is used as a reactor for gas distribution at the bottom. A secondary 80 mL quartz reactor with the same micropore design is also employed (Fig. 2).

To ensure precise monitoring and control of the CO_2 capture and syngas production processes, a suite of industrial-grade sensors was integrated into the experimental setup. These sensors provided real-time data on gas composition, solvent integrity, catalyst bed temperature, and gas flow rates. The specifications of the integrated sensors used are summarized in Table 1. Each sensor was calibrated before experimentation, and data were logged at one-second intervals to generate high-resolution profiles of capture kinetics and catalytic performance.

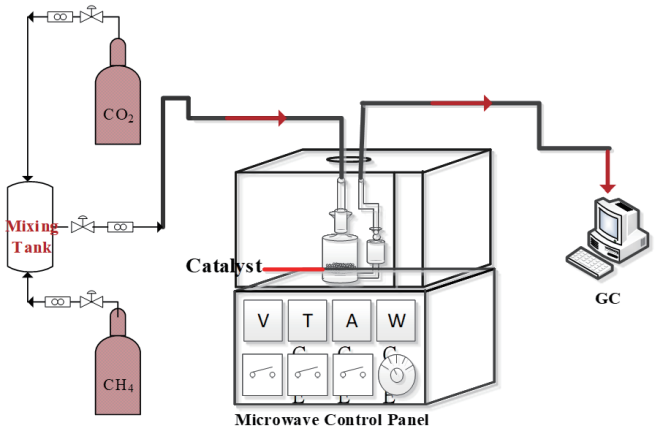

Fig. 2. (Color online) Schematic diagram of syngas production equipment.

Table 1
Specifications of sensors used in CO_2 capture and syngas production systems.

Specification	NDIR sensor	Conductivity sensor	Thermocouple sensor	MFC
Model	Cubic Gasboard 2051 /Alphasense IRC AT	Yokogawa SC42 P S/ Hach CDC401	K type (NiCr-NiAl)	Alicat M Serie/ Bronkhorst EL FLOW Select
Measurement range	CO_2: 0–10% vol; CH_4: 0–3500 ppm	0–200 mS/cm	−200 °C to +1250 °C	0–500 sccm to 0–20 L/min
Accuracy/resolution	±1% FS; Resolution 0.001% vol CO_2	±0.5% of reading	±1.5 °C or ±0.4% of reading	±0.8% of reading ±0.2% FS
Operating condition	0–45 °C; 0–90% RH (noncondensing)	0–100 °C	Gas phase and microwave reactor conditions	0–10 bar
Output/interface	UART (TTL/RS 232)	4–20 mA analog/ Modbus digital	mV analog to PID controller	RS 232/Modbus/ Analog 4–20 mA
Application	Inlet/outlet CO_2 and CH_4 concentration monitoring	Alkali solution concentration and degradation monitoring	Catalyst bed and contact tank temperature control	Precise control of CH_4 and CO_2 feed ratios

2.2 Analysis and sensing

The CO_2 capture efficiency was monitored using an integrated gas sensing array. An NDIR sensor was used to measure inlet and outlet CO_2 concentrations within a range of 0–25000 ppm with an accuracy of ±2%. MFCs equipped with thermal flow sensors were employed to regulate methane (CH_4) and CO_2 gas streams. A K-type thermocouple sensor was used to measure the waste Pt catalyst bed temperature after microwave irradiation. Conductivity sensors were used to monitor alkali solution concentration and degradation. The chemical transformation of the NaOH solution during CO_2 absorption was monitored using integrated electrochemical sensors. The solution's pH was measured using a high-sensitivity glass electrode pH sensor (Orion™ 8102BNUWP ROSS Ultra™, Thermo Fisher Scientific, USA) with an accuracy of 0.01 pH units, calibrated across a range of pH 7–14. The electrical conductivity (EC) of the absorbent was monitored using a platinum-electrode conductivity sensor (nPro 7108/25/40 with a 4-pole conductivity sensor, Mettler Toledo, Switzerland) with a measurement range of 0–200 mS/cm. EC and pH sensors were submerged in the gas-liquid contact tank to ensure real-time data acquisition, with measurements recorded at 1 min intervals throughout the reaction cycle.

2.3 Experiment

The alkali carbon capture experiment was conducted in continuous batch mode with a circulation rate of 480 ml/min. CO_2 concentrations ranged between 14500 and 14800 ppm, and alkali absorption solution concentrations were varied to 1, 3, 5, and 7%. For syngas production, 6 g of waste Pt catalyst and 0.8 g of micron-sized iron powder were placed in the reactor. The microwave power was set at 450 W with a total exposure time of 240 min. The feed composition was set to 10/10 ml/min (CH_4/CO_2). After 60 min of system stabilization, gas samples were collected every 30 min using a 1 ml airtight syringe. The syngas yield was calculated on the basis of the results of a carbon mass balance analysis. The chemical composition of intermediates and products was analyzed with a gas chromatograph equipped with a thermal conductivity detector (GC-TCD, SHIMADZU GC-2014). The tail gas composition was analyzed by gas chromatography, with a 1 μl sample collected every 60 min in triplicate. The coke content of the catalyst was determined using a carbon determinator (Eltra, CS 800).

3. Results

3.1 Monitoring performance of sensors

The CO_2 absorption process proceeds through consecutive reaction steps, forming sodium carbonate (Na_2CO_3) and sodium bicarbonate ($NaHCO_3$). Within the Na_2CO_3 production range, the reaction rate and capture efficiency are strongly dependent on the NaOH concentration. In this study, an integrated NDIR gas sensor enabled the continuous, real-time monitoring of CO_2 concentration data, enabling the high-resolution analysis of breakthrough kinetics. The breakthrough time is defined as the time at which the effluent gas concentration (C) reaches a

predetermined fraction, typically 5–10% of the inlet concentration (C_0). This point indicates that the absorbent capacity has approached exhausion. A breakthrough curve (Figs. 3 and 4) illustrates the C/C_0 ratio over time. In the figures, a steeper curve indicates faster saturation, whereas a delayed breakthrough implies greater absorbent capture capacity. The real-time monitoring of this point using high-precision sensors is essential for determining the operational lifespan of the NaOH solution and evaluating the efficiency of the waste Pt catalyst.

The kinetic properties recorded by the sensing system are summarized in Table 2. The data revealed a sharp decrease in CO_2 level within the first 120 s of exposure, confirming high initial reactivity. The sensitivity of the NDIR sensor was sufficient to detect minor fluctuations in capture rates, often attributed to localized temperature gradients within the absorbent bed. As shown in Fig. 5, CO_2 absorption efficiency increased significantly with NaOH concentration.

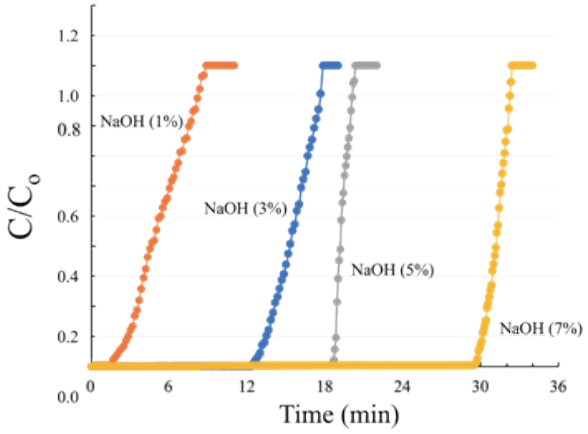

Fig. 3. (Color online) Breakthrough curves of CO_2 adsorption using NaOH solutions at different concentrations (1, 3, 5, and 7%). Higher NaOH concentrations delay breakthrough, indicating enhanced absorption capacity.

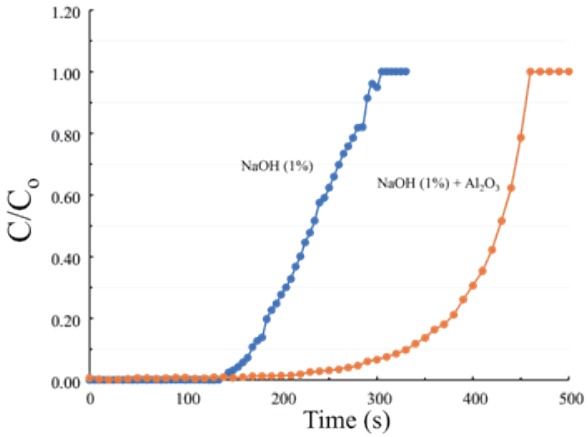

Fig. 4. (Color online) Breakthrough curves of CO_2 adsorption in 1% NaOH solution with and without α-Al_2O_3 addition, which delay breakthrough, demonstrating improved adsorption performance.

Table 2
Breakthrough times and absorption efficiencies of sensors in various NaOH concentrations.

NaOH concentration (%)	Breakthrough time (s)	Time to reach 90% efficiency (s)
1	138	240
3	750	200
5	1116	150
7	1782	70

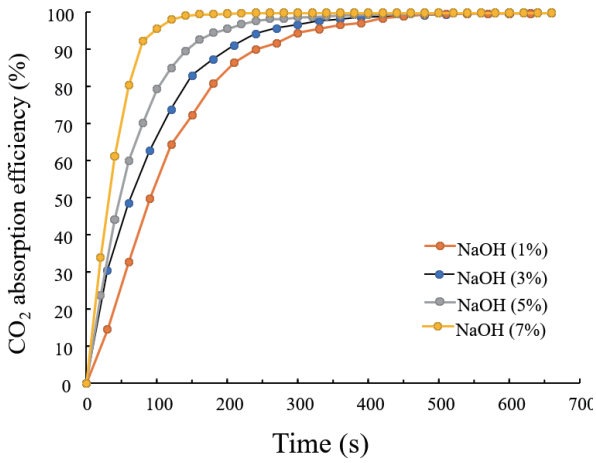

Fig. 5. (Color online) Relationship of CO_2 adsorption efficiency for NaOH solutions (1, 3, 5, and 7%).

From a thermodynamic perspective, the complete conversion of NaOH is theoretically consistent with an adiabatic process, implying that capture capacity depends primarily on the molar quantity of NaOH available for neutralization. Figure 3 shows the effect of α-Al_2O_3 addition to 1% NaOH solution. The delayed breakthrough curve confirms that α-Al_2O_3 enhances adsorption capacity by extending the effective lifespan of the absorbent. This highlights the importance of sensor-based monitoring in detecting subtle improvements in system performance.

3.2 Impact of α-Al_2O_3 on absorption kinetics

Gas–liquid contact area is a decisive factor in CO_2 capture. The addition of α-Al_2O_3 spheres transforms the single gas–liquid interface into a multi-point dispersed contact pattern. This alteration of the flow field, monitored using integrated mass flow sensors, enhances the effective contact area and ensures a more uniform CO_2 transfer to the liquid phase. The results presented in Fig. 4 show that at a NaOH concentration of 1%, the addition of 100 g of α-Al_2O_3 (in 0.3 cm diameter) extended the CO_2 adsorption breakthrough time from 138 to 750 s. The integration of flow sensors enabled the calculation of this breakthrough point with a significantly higher precision than manual sampling methods, as continuous data were used to capture the exact moment of solvent saturation.[12]

3.3 EC and pH

The transformation of CO_2 into ionic species (CO_3^{2-} and HCO_3^-) was monitored using submerged electrochemical sensors to obtain detailed insights into the reaction's ionic dynamics. The pH data shown in Fig. 6 represent the shifting ionic equilibrium during CO_2 absorption. Initially, at $pH > 11$, CO_3^{2-} formation dominates, corresponding to the high alkalinity of the NaOH solution. As the reaction progresses and alkalinity decreases, HCO_3^- becomes the primary species, marking the transition toward bicarbonate stabilization. EC measurements show a distinct decline in solution conductivity (Fig. 6), primarily attributed to the depletion of hydroxide (OH^-) ions and their gradual replacement by carbonate (CO_3^{2-}) ions, which exhibit lower ionic conductivity e (55 $S \cdot cm^2/mol \cdot z$).[13] The high-frequency sampling rate of the EC sensor captured this transformation with exceptional temporal resolution, producing a distinctive chemical signature of the reaction progress.

Real-time electrochemical monitoring enables the quantitative validation of the CO_2 capture neutralization mechanism. The synchronized EC and pH data revealed the kinetics of ionic conversion, enabling the precise determination of the reaction endpoint and absorbent exhaustion. The sensors were also used for the dynamic adjustment of NaOH concentration and reaction time to optimize CO_2 uptake.

3.4 Syngas production and catalyst monitoring

The catalytic performance of waste Pt was evaluated through microwave-assisted dry reforming, with integrated sensor systems used to monitor reaction conditions and product yields. The H_2 and CO yields were monitored for 240 min using GC and flow sensors. The addition of high-dielectric iron particles to the γ-Al_2O_3-supported Pt catalyst enhanced microwave coupling by converting electromagnetic energy into thermal energy for syngas production. Localized microwave absorption by iron particles and carbon deposition may induce transient hot spots and occasional spark phenomena during irradiation.

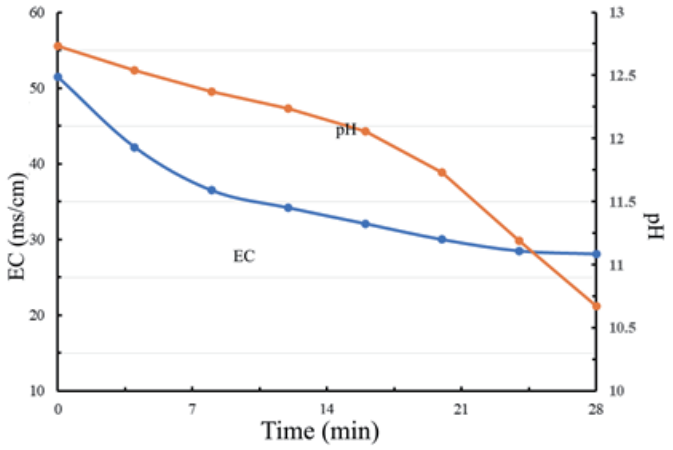

Fig. 6. (Color online) Relationship between solution conductivity and pH during CO_2 adsorption in 3% NaOH.

Figure 7 illustrates the role of sensor systems in monitoring process stability. Under a CH_4/CO_2 flow ratio of 10/10 mL/min, the waste Pt catalyst maintained stable CO_2 conversion, with average H_2 and CO yields of 18.8 and 25.1%, respectively. A K-type thermocouple was used to monitor the catalyst bed temperature during microwave-assisted reforming. The microwave reactor was operated under a power-controlled PID mode with a fixed input power of 450 W, where PID regulation maintained stable microwave output power rather than temperature-based feedback control. The observed transient hot spots were associated with localized microwave heating and carbon deposition, as confirmed by the carbon accumulation of 12.3 wt%.

3.5 Catalyst surface characterization

The surface morphology and elemental composition of the waste Pt catalyst before and after microwave-assisted reaction were characterized by FE-SEM and EDS, respectively. As shown in Fig. 8, Pt, Al, O, and C elements were detected. The Al and O signals are mainly attributed to the γ-Al_2O_3 support, whereas the Pt signal confirms the presence of platinum species. The detected C indicates the formation of carbonaceous species on the catalyst surface during the reaction. The carbon content increased from 1.4 wt% before reaction to 12.3 wt% after microwave-assisted conversion, indicating enhanced carbon deposition. As shown in Fig. 9, the reacted catalyst exhibited denser carbonaceous deposits on the surface [Fig. 9(b)] compared with the untreated catalyst [Fig. 9(a)], suggesting the formation of methane-derived carbon species during

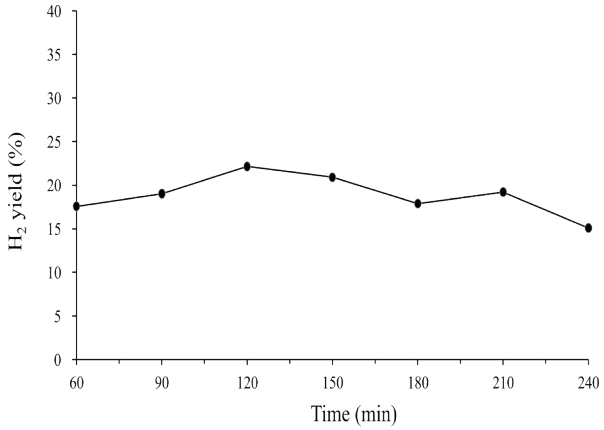

Fig. 7. H_2 yield of dry reforming using waste Pt catalyst for 240 min.

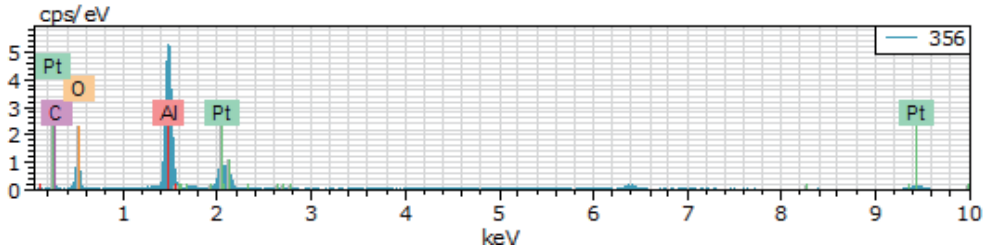

Fig. 8. (Color online) EDS spectrum and elemental composition of the waste Pt catalyst.

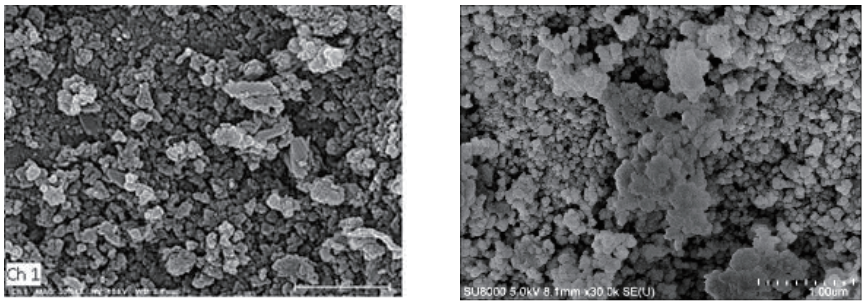

(a) (b)

Fig. 9. SEM images of the waste Pt catalyst (a) before and (b) after microwave treatment. The scale bar represents 1 μm, and images were obtained at 30000× magnification.

the reaction. The deposited carbon may affect Pt active-site accessibility and modify the local dielectric properties of the catalyst bed, thereby affecting microwave absorption and localized heating behavior.

4. Discussion

The integration of high-precision NDIR gas sensors and MFCs in CCU provides essential data to understand CO_2 absorption kinetics. Sensors enable the capture of rapid saturation phenomena and the identification of breakthrough times ranging from 138 to 1782 s at different NaOH concentrations. The ability to log data every 1 s allows for the precise calculation of the 90% adsorption efficiency milestones (70–240 s). The results of this study validate the importance of NDIR technology in high-humidity, high-concentration greenhouse gas environments. The robustness of the NDIR profile against minor pressure fluctuations during CO_2 absorption confirms that optical sensing is ideal for automated control in industrial-scale alkali-based capture systems.[9]

By synchronizing pH and EC data, the exact shift from CO_3^{-2} dominance at pH > 11 to HCO_3^- dominance at pH of 7–10 was identified. The observed EC decrease is driven by the 3.6-fold difference in equivalent conductivity between the depleted OH^- (98.6 S·cm^2/mol·z) and the generated carbonate (CO_3^{2-}, 55 S·cm^2/mol·z), serving as a predictive metric for solvent exhaustion. This relationship demonstrates that conductivity sensors act as a low-cost, durable alternative to expensive gas analyzers for monitoring the health of a NaOH absorbent. This sensing approach, where ionic shifts in the liquid phase indicate conversion efficiency in the gas phase, advances the development of simplified, automated feedback for the chemical scrubbing towers of CO_2.

In this study, syngas production through microwave-assisted dry reforming is challenging for sensing technologies. The environment in the reactor is characterized by high electromagnetic interference and localized thermal hotspots generated by the iron dielectric medium. In this study, effluent gas sensors are used to monitor catalytic performance even when the reactor is subjected to 450 W of microwave power. The stable yields of H_2 (18.8%) and CO (25.1%) measured for 240 min show that the waste Pt catalyst maintains its integrity under sensor-

monitored conditions. The stable H_2/CO ratio close to 1 indicates that integrated flow and gas sensors effectively manage coke deposition (12.3 wt%) by facilitating real-time adjustments to the CH_4/CO_2 feed ratio.[10] Such results contribute to the development of smart reactor systems where sensor feedback mitigates catalyst deactivation during the utilization of recycled materials.

By utilizing waste Pt and alkaline solutions, waste-to-value cycles are achieved. Unlike conventional studies using fresh commercial Pt catalysts, this work focuses on the recovery, modification, and reuse of industrial waste Pt catalysts as value-added catalytic materials for syngas production. Although a direct comparison with commercial Pt catalysts was not included in this study, the obtained results demonstrate the catalytic potential of recycled Pt materials and provide a sustainable approach for catalyst regeneration and resource utilization. In the cycle, sensors are essential to handle the inherent variability of recycled catalysts and absorbents, transforming an unpredictable chemical waste stream into a precision-controlled manufacturing process for syngas. Sensor technology enables the discovery of kinetic and ionic thresholds while advancing simple monitoring to the essential component of sustainable carbon management systems.[8] Although the present study was conducted at a laboratory scale, the obtained results demonstrate the feasibility of the proposed CO_2 capture process. However, further evaluation is required for industrial-scale implementation, including pilot-scale validation, the optimization of mass transfer efficiency, energy consumption, and long-term operational stability. Future work will focus on addressing these aspects to evaluate the practical feasibility of the proposed system for industrial applications.

5. Conclusions

A closed-loop system was developed in this study for carbon capture and syngas production for CO_2 utilization using NaOH absorbents and waste Pt catalysts under microwave induction. By incorporating micron-sized iron as a high-dielectric medium (14.2 F/m), the system effectively converts microwave energy into thermal energy, overcoming the thermal limitations of the catalyst carrier. A bidirectional relationship between sensing technology and CCU is validated in this study. The employment of NDIR sensors enables the precise identification of CO_2 breakthrough times at 138, 750, 1116, and 1782 s, validating the robustness of optical sensing in high-concentration CO_2 environments. Electrochemical sensors contribute to the development of sensing-by-proxy models, where real-time pH and EC data are used to predict the transition from Na_2CO_3 to $NaHCO_3$ production, offering a low-cost alternative for monitoring solvent status. The results also show how interface materials such as α-Al_2O_3 extend breakthrough times by 108% through multi-point contact patterns. Finally, syngas yields confirm that integrated sensor data utilization contributes to mitigating catalyst deactivation issues, such as coke deposition, by facilitating real-time feed adjustments. The results of this study present the evolution of smart reactors through the integration of sensor technology to transforming unstable CO_2 capture and utilization into stable industrial processes for sustainable resource management.

References

1 T. T. H. Hoang, S. Verma, S. Ma, T. T. Fister, J. Timoshenko, A. I. Frenkel, P. J. A. Kenis, and A. A. Gewirth: J. Am. Chem. Soc. **140** (2018) 5791. https://doi.org/10.1021/jacs.8b01868
2 C. Tangsathitkulchai, S. Naksusuk, A. Wongkoblap, P. Phadungbut, and P. Borisut: Processes **9** (2021) 201. https://doi.org/10.3390/pr9020201
3 E. O. Otieno, R. Kiplimo, and U. Mutwiwa: Heliyon **27** (2023) e14041. https://doi.org/10.1016/j.heliyon.2023.e14041
4 A. Cabello, T. Mendiara, A. Abad, and J. Adánez: Energy Convers. Manag. **267** (2022) 115865. https://doi.org/10.1016/j.enconman.2022.115865
5 C. Y. Chiang, D. W. Lee, and H. S. Liu: J. Taiwan Inst. Chem. Eng. **72** (2017) 29. https://doi.org/10.1016/j.jtice.2017.01.023
6 J. G. Shim, D. W. Lee, J. H. Lee, and N. S. Kwak: Environ. Eng. Res. **21** (2016) 297. https://doi.org/10.4491/eer.2016.042
7 A. L. Silva-Gálvez, A. López-Sánchez, M. A. Camargo-Valero, F. Prosenc, M. E. González-López, and M. S. Gradilla-Hernández: J. Environ. Manag. **354** (2024) 120258. https://doi.org/10.1016/j.jenvman.2024.120258
8 W. Wang, N. Wei, F. Wei, M. Ali, K. Lin, and S. Lei: J. Clean Prod. **529** (2025) 146826. https://doi.org/10.1016/j.jclepro.2025.146826
9 J. C. Heldens, T. Koturbash, J. Fridh, and J. Östlund: Fuel **402** (2025) 135860. https://doi.org/10.1016/j.fuel.2025.135860
10 C. Luo, Y. Chen, A. Braniff, M. A. Al Masud, Y. Tian, B. K. Desta, Y. Wang, and J. Hu: Chem. Eng. J. **533** (2026) 174878. https://doi.org/10.1016/j.cej.2026.174878
11 W. J. Jeon and M. G. Lee: J. CO2. Util. **106** (2026) 103405. https://doi.org/10.1016/j.jcou.2026.103405
12 X. Fan, X. Li, W. Zhang, P. Lian, G. Mi, H. Guan, Y. Wang, Y. Su, H. Tai, Y. Jiang, and W. Li: Infrared Phys. Technol. **152** (2026) 106190. https://doi.org/10.1016/j.infrared.2025.106190
13 W. Guo, C. Wang, J. Wang, J. Xu, W. Li, and D. Zhang: Chem. Sep. Purif. Technol. **383** (2026) 136143. https://doi.org/10.1016/j.seppur.2025.136143